

## Research Article

# Differentiating Middle Ear and Medial Olivocochlear Effects on Transient-Evoked Otoacoustic Emissions

KENDRA L MARKS<sup>1</sup> AND JONATHAN H SIEGEL<sup>1</sup>

<sup>1</sup>*Department of Communication Sciences and Disorders, School of Communication, Northwestern University, 2240 Campus Drive, Evanston, IL 60208-2952, USA*

Received: 23 April 2016; Accepted: 22 March 2017; Online publication: 21 April 2017

## ABSTRACT

The response of the inner ear is modulated by the middle ear muscle (MEM) and olivocochlear (OC) efferent systems. Both systems can be activated reflexively by acoustic stimuli delivered to one or both ears. The acoustic middle ear muscle reflex (MEMR) controls the transmission of acoustic signals through the middle ear, while reflex activation of the medial component of the olivocochlear system (the MOCR) modulates cochlear mechanics. The relative prominence of the two efferent systems varies widely between species. Measuring the effect of either of these systems can be confounded by simultaneously activating the other. We describe a simple, sensitive online method that can identify the effects both systems have on otoacoustic emissions (OAEs) evoked by transient stimuli such as clicks or tone pips (TEOAEs). The method detects directly in the time domain the changes in the stimulus and/or emission pressures caused by contralateral noise. Measurements in human participants are consistent with other reports that the threshold for MOCR activation is consistently lower than for MEMR. The method appears to control for drift and subject-generated noise well enough to avoid the need for post hoc processing, making it promising for application in animal experiments (even if awake) and in the hearing clinic.

**Keywords:** otoacoustic emissions, transient-evoked, contralateral noise, olivocochlear, acoustic reflex

## INTRODUCTION

The response of the peripheral auditory system to sound is modulated by two efferent neural pathways. Contraction of either the stapedius or tensor tympani muscle attenuates sound transmission through the middle ear and reduces the fraction of the sound intensity incident on the eardrum that reaches the inner ear. In humans, the acoustic middle ear muscle reflex (MEMR) primarily activates the stapedius muscle (Møller 2012). There has been much interest in the medial component of the olivocochlear (MOC) system and its sound-activated reflex (the MOCR), because it influences the gain of the cochlear amplifier (Murugasu and Russell 1996; Dolan et al. 1997; Cooper and Guinan 2003). This action via axosomatic synaptic contacts on the outer hair cells with spatially restricted innervation suggests that gain control may be specific to different cochlear places. The two pathways appear to have important behavioral significance, including optimizing the dynamic range of hearing. The olivocochlear system appears to play a role in selective attention (Delano et al. 2007) and optimize hearing in the presence of interfering noise (Winslow and Sachs 1987) (reviewed by Robles and Delano 2008; Guinan 2010) and may slow cochlear aging (Liberman et al. 2014).

Both the MEMR and MOCR influence the levels of otoacoustic emissions (OAEs) in the ear canal (Mountain 1980; Siegel and Kim 1982; Collet et al. 1990; Guinan et al. 2003; Guinan 2006). The MEMR affects both the inward travel of stimulus signals to the cochlea as well as the outward propagation of OAE signals. Along with its effect on the cochlear amplifier, the MOC system reduces intracochlear generation of OAEs. Differences between individual subjects are

---

*Correspondence to:* Jonathan H Siegel · Department of Communication Sciences and Disorders, School of Communication · Northwestern University · 2240 Campus Drive, Evanston, IL 60208-2952, USA. Telephone: (847) 491-2454; email: j-siegel@northwestern.edu

seen in the strength of both reflexes (Backus and Guinan 2007; Goodman et al. 2013; Marshall et al. 2014; Xu et al. 2015). Evidence that the strength of one or both of these efferent pathways may be reduced following damage to the cochlear sensory neurons (Maison and Liberman 2000; Maison et al. 2013; Valero et al. 2016) adds further impetus to study both pathways. The MEMR has been exploited as a clinical diagnostic test of cochlear and brainstem integrity (reviewed by Møller 2012). While the effect of the MOCR on OAEs in humans was first reported more than 25 years ago (Collet et al. 1990), the phenomenon has not been widely applied in the clinic despite its potential usefulness, such as detecting auditory neuropathy (Hood et al. 2003). One contributing factor is uncertainty over whether attempts to measure the MOCR are sometimes contaminated by the MEMR. An efficient method for differentiating MEMR and MOCR effects could increase the usefulness of both in clinical tests.

The threshold for activating the MOCR has been found to be consistently lower than the threshold for activating the MEMR in cats (Liberman et al. 1996), but this is not the case for rats (Relkin et al. 2005), rabbits (Whitehead et al. 1991), and mice (Xu et al. 2015, 2017; Valero et al. 2016). These studies in animals were likely influenced by anesthesia, which is the subject of the companion paper (Xu et al. 2017). Even in humans, the thresholds for activating the MEMR and MOCR vary between individuals. Activation of the MEMR can be detected in some humans at levels well below the thresholds determined with the standard MEMR assessment used in the clinic: a change in immittance visually detected using a tympanometer. For example, a measure of wideband reflectance was reported to detect reflex thresholds as much as 24 dB below the clinical measure (Feeney et al. 2003). Small changes in the response to a low-frequency probe also indicate an MEMR below typical clinical thresholds (Goodman and Keefe 2006; Deeter et al. 2009; Zhao and Dhar 2010, 2011). At least some of the reports of unusually low MEMR thresholds may have been compromised by the presence of otoacoustic emissions, which can be modulated by the MOCR (Keefe et al. 2010, 2017). Consequently, measurements of the peripheral effects of either efferent pathway require differentiating MEMR and MOCR activation, as either one may contaminate measurements of the other.

It is thus important to assess the conditions of acoustic stimulation that may selectively activate either the MEMR or MOCR. The influence of the MOCR grows with increasing intensity of sound presented to either the contralateral or ipsilateral ear, but it is not possible to quantify the effect of full activation of the

MOCR if the eliciting sound also activates the MEMR. The MEMR can be blocked in laboratory experiments on animals by surgical interruption of the tendons of the middle ear muscles (Siegel and Kim 1982; Wolter et al. 2014), blocking or severing their motor inputs (Songer and Rosowski 2005), or by systemic application of a paralytic agent (Mountain 1980). These manipulations are not possible in human subjects, so alternate methods are needed.

We have developed a relatively simple method to detect changes in otoacoustic emissions evoked by short acoustic tone pips (generally referred to as transient-evoked otoacoustic emissions (TEOAEs)) that shows promise to be developed into a reliable tool for the research lab or hearing clinic. A brief report of this work has appeared in abstract form (Marks and Siegel 2011).

## METHODS

### Participants

Fourteen normal hearing adults (8 females), ranging in age from 18 to 22 years, participated in this study. Otoscopy, tympanometry, and clinical MEMR threshold tests were performed to ensure normal outer and middle ear function. Both ears were screened. One ear was chosen at random for threshold and otoacoustic emission measurements. Behavioral thresholds were measured from 0.125 kHz to the upper limit of each participant's hearing range using Békésy tracking and automated detection of threshold convergence as described previously (Lee et al. 2012). All had thresholds at all frequencies within 15 dB of average thresholds for this age group. TEOAEs evoked by tone pips (see below) were also measured in all 14 participants. We measured changes in the TEOAEs during presentation of broadband noise to the contralateral ear in 10 participants. One participant showed no evidence of an MEMR at a contralateral noise level of 100 dB SPL, the highest level tested. If any abnormalities appeared during this initial testing, the participant was paid for their time and dismissed. During testing, the participants watched a movie of their choice, muted audio with subtitles. This kept the participants awake and reasonably quiet, and they maintained a fairly steady head position while reading the subtitles. All measurements other than tympanometry were made with the participant seated quietly in a double-walled sound booth (Industrial Acoustics Corp.). Human subject protocols were approved by the Northwestern University Institutional Review Board.

## Instrumentation

Conventional middle ear assessment used an Interacoustics AA220 tympanometer. The level of the 226-Hz probe tone was measured as 85.6 dB SPL when the probe was inserted into a 60318-4 ear simulator to a depth similar to that used for testing in real ears. Measurements of TEOAEs and behavioral thresholds used custom software written in Visual Basic 6.0 running on a PC with an Echo Gina 3G 24-bit digital audio interface. The sample rate for TEOAE measurements was 88.2 kHz and 44.1 kHz for threshold tracking. An Etymotic Research ER-10B+ otoacoustic emission probe (preamplifier gain set to +20 dB) was sealed into one ear using an ER10-14 disposable foam ear tip. The sound source transducers were modified MB Quart 13.01 HX coupled to the emission probe via flexible 16-ga plastic tubing. These transducers are much more linear than the tube phones typically used for the ER-10B+, allowing TEOAEs to be separated from the stimulus pressure as described below. The depth of insertion of the emission probe was assessed by measuring the frequency of the first half-wave resonance (Souza et al. 2014). Pressure responses to chirp excitation were measured using either SYSRES (version 2.24) (Neely and Stevenson 2002) or EMAY (version 3.03) (Neely and Liu 1994) at a level of nominally 80 dB SPL. SYSRES was also used to screen for spontaneous OAEs using spectral averaging (50 spectral averages using a 65,532-point buffer sampled at 32 kHz yielding a spectral resolution of 0.49 Hz). Contralateral noise was delivered using an ER-3A tube phone.

The emission probe microphone transfer function was measured as described previously (Siegel 2002; Rasetshwane and Neely 2011) and used to compensate the measured responses in the frequency domain, with the result transformed back to the time domain using an inverse FFT. To properly interpret the emission delays, all system delays must be measured and compensated, including the constant delay between the start of digital-to-analog and analog-to-digital conversion of the digital audio interface and the acoustic delays of the sound sources and microphone transfer function. The sum of the D/A to A/D and sound source acoustic delays were compensated by subtracting a constant delay of 1.92 ms from the time waveform. Proper delay compensation was verified in the frequency domain representation of the probe stimulus, which showed invariant phase with frequency (see the example in Fig. 5c). This approach to compensating system delays has been verified by comparing the group delays of TEOAE and stimulus-frequency otoacoustic emissions (SFOAE) measured in the same individual (Siegel et al. 2011).

## TEOAE Measurement

TEOAEs were measured using custom software and a scale and subtract (compression) method to separate the emission from the stimulus (Kemp and Chum 1980; Siegel et al. 2011). The OAE-evoking stimuli were 2-ms cosine-gated tone pips (no steady-state) centered at 2, 3, or 4 kHz, and the frequency evoking the largest emissions was selected for further study. Like the conventional “nonlinear” paradigm to measure TEOAEs (Kemp et al. 1986), this method relies on the observation that OAEs generally grow compressively with increasing stimulus level. On the other hand, the emission probe and sound sources exhibit sufficiently close to linear behavior that the stimulus exhibits approximately linear growth with increasing drive level. Our implementation of the nonlinear paradigm uses improved instrumentation and selection of stimulus levels that yield a measure of the TEOAE that is likely to be closer to a linear separation between the stimulus and emission pressures.

In operation, the system presents four tone pips at a defined peak equivalent SPL (the “probe” with amplitude  $A_{\text{probe}}$ ) followed by a more intense tone pip (the “reference” with amplitude  $R \cdot A_{\text{probe}}$  with  $R > 1$ ). The amplitude of the reference stimulus is made high enough so that the emission is at least partly saturated but not high enough to evoke the MEMR or drive the system outside its linear range. If these conditions are met, the response to the reference stimulus is relatively uncontaminated by the OAE and can be presumed to be dominated by the stimulus pressure. If this assumption is valid, then scaling down the response to the reference stimulus by factor  $R$  provides a good estimate of the probe stimulus pressure. Subtracting this stimulus pressure estimate from the response to the probe should then yield a more accurate estimate of the TEOAE than the nonlinear method. The basis for this assertion is found in the “compression” method of extracting SFOAEs demonstrated by Kalluri and Shera (2007).

In all cases, the probe and reference pips, interleaved as described below, were presented at a repetition rate of 21.533 Hz at 50 and 70 dB peak equivalent SPL (peSPL), respectively. The peak voltage delivered to the sound source at each probe frequency was determined using the depth-compensated ear simulator method described previously (Lee et al. 2012; Souza et al. 2014). As the sound sources were well-equalized, the entire spectrum of the pip stimuli was not compensated. The 50-dB peSPL probe tone pips at this repetition rate would not be expected to influence the MOCR; indeed, clicks presented at 55 dB peSPL were found not to influence MOC effects for rates below 31.25 Hz (Boothalingam and Purcell 2015). However, the 70-

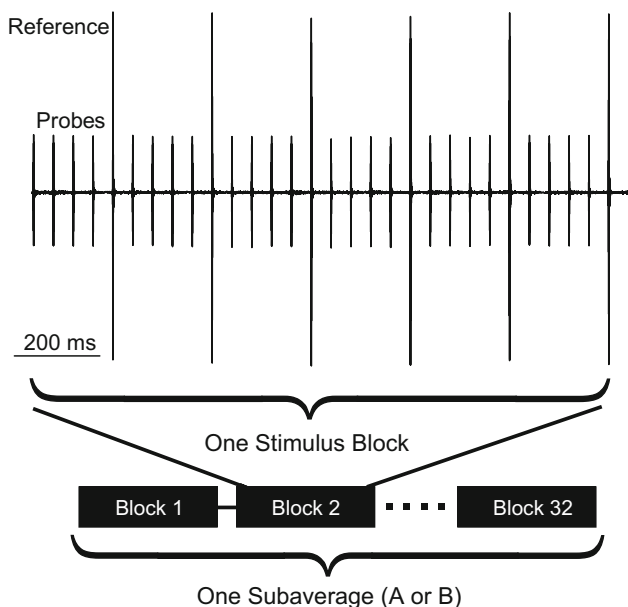


**FIG. 1.** Time record of TEOAE measurement using the scale-subtract (compression) method. In this example, the amplitude of the reference stimuli was 10 dB greater than that of the probe stimuli. Each stimulus block shown here is used to calculate the OAE residual from the averages of the probe and reference responses, tested for contamination by noise. This sequence is repeated 32 times to calculate one of two subaverages.

dB peSPL reference pips may activate the MOCR (Guinan et al. 2003).

Trains of 4 probe stimuli, followed by one reference stimulus were repeated 6 times to comprise one block of 24 probe and 6 reference pips (1393.2 ms) (Fig. 1).<sup>1</sup> Responses to the probe and reference stimuli were averaged separately. The probe's stimulus pressure (i.e., with minimal contribution from the TEOAE) was estimated by scaling down the averaged response to the reference pip by the ratio of amplitudes of the reference and probe stimuli ( $R$ ). The average of the responses to the probe stimuli contained the TEOAE plus the probe stimulus pressure. Subtracting the probe-stimulus-pressure-estimate from the averaged response to the probe yielded the TEOAE residual. The adequacy of system linearity was judged by the degree of cancellation of the probe stimulus pressure, with no artifact typically observable above the system noise.

An online noise rejection algorithm was then applied to the OAE residual calculated from each stimulus block to determine whether it should be accepted. An accepted block passed two criteria: it must not exceed either (1) a specified total rms pressure or (2) a specified peak pressure. The two

criteria were adjusted by the experimenter based on the movement-related noise of the individual subject and stimulus frequency. This algorithm was very effective in practice, particularly when the rejection criteria were set to reject ~10–20 % of the total number of block averages when the subject was generally quiet (suggested by D. Keefe, private communication). Because the stimulus pressure is canceled, leaving only the TEOAE typically at least 20 dB below the amplitude of the stimulus pips, performing the noise rejection test on the residual allows even small levels of contaminating noise to be detected. The residuals from each accepted stimulus block were accumulated in a memory buffer until the desired number of probe stimuli (32 repetitions of 24 = 768) had been delivered. This constitutes one subaverage. The subaverage was repeated, doubling the total number of probe presentations (1536). The two resulting subaverages of the TEOAE residual (denoted averages A and B) were averaged to yield the grand average  $((A + B)/2)$  and this time average represented the “signal” buffer. Subtracting the two time averages  $((A - B)/2)$  yielded a “noise” buffer that was used to estimate the noise floor, which also reveals artifacts generated in either of the two duplicate subaverages. This approach to calculating signal and noise buffers has been used previously (Kemp et al. 1990; Gorga et al. 1993; Goodman et al. 2013). Each TEOAE measurement took ~2.5 min. An example of the TEOAE evoked by 4 kHz tone pips at 50 dB peSPL (70 dB peSPL reference) is shown in Figure 2. This figure illustrates better than 1000:1 cancellation of the stimulus pressure, as there is no visible stimulus artifact

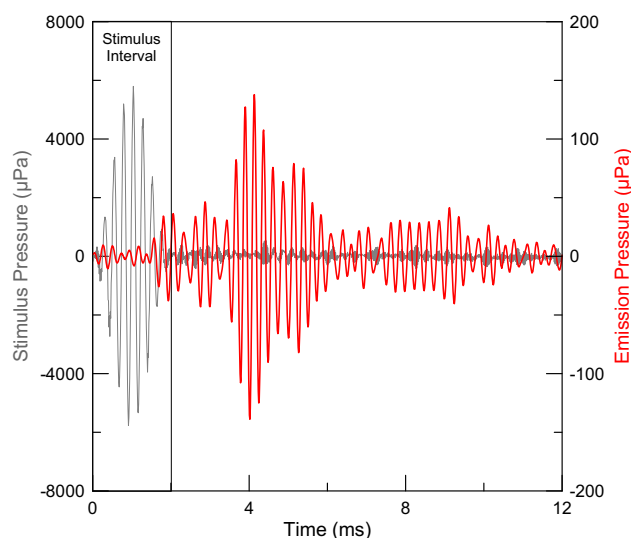


**FIG. 2.** TEOAE (red) evoked by 4 kHz tone pips (gray) at 50 dB peSPL, separated from the stimulus pressure using a 70-dB peSPL reference (note the 400:1 difference in pressure axis scaling). Cancellation of the stimulus artifact (red curve, first 2 ms) is better than 1000:1.

<sup>1</sup> The response to an additional set of 4 probe and 1 reference pips was not included in the averaging in case of onset artifacts. As none were detected, this step was probably not necessary.



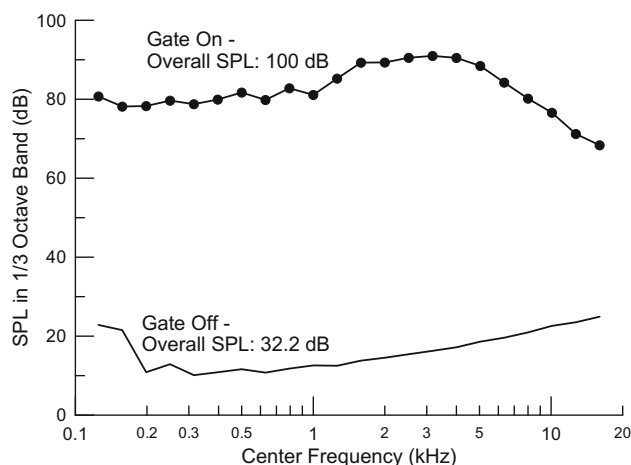


**FIG. 3.** Spectral content of contralateral noise generated by the ER-3A insert earphone for the highest available level. *Line at the bottom* depicts the greatly attenuated noise with the electronic gating switch turned off.

above the system noise. Calculating the TEOAE residual using interleaved probe and reference stimuli had the added benefit of minimizing the effects of slow drift in stimulus levels (Backus 2007; Backus and Guinan 2007; Goodman et al. 2013).<sup>2</sup>

### Effects of Contralateral Noise

The contralateral noise (Fig. 3) used an analog random pink noise generator (Altec 8080A) gated by an electronic switch controlled by the computer and delivered to an Etymotic Research ER-3A insert earphone. Most previous studies have used white noise, but we prefer the constant power/octave feature of pink noise (Fig. 3) that should produce more constant excitation of the basilar membrane vs distance. Noise levels were calibrated with the end of the ear tip positioned at the reference plane of the Bruel and Kjaer 4157 ear simulator as specified in standards (ANSI S3.25-2009; IEC 60318-4, 2010).

A simple procedure was used to measure the contralateral-noise-induced changes in the tone pip response by detecting changes in the time interval of either the stimulus or the TEOAE, presumably representing activation of the MEMR or MOCR, respectively. The OAE probe delivered trains of 18 probe stimuli (835.9 ms duration) with no reference stimuli, and the responses to the last 16 probe stimuli were averaged. The noise was then gated on for

592.9 ms to allow sufficient time for activation of MEMR and MOC pathways before a second average of responses to an identical set of probe stimuli was collected as described for the no-noise condition (Fig. 4). The contralateral noise was then gated off for 592.3 ms before the next pair of measurements to allow the contralateral effects to dissipate. Both efferent effects have rise and fall times of  $\sim 200$  ms in humans (Borg 1982; Backus and Guinan 2006). The MEMR shows pronounced adaptation (reflex decay), but the MOCR exhibits relatively little adaptation (Relkin et al. 2005; Backus and Guinan 2006). The change in the ear canal pressure was then calculated by subtracting the two time averages with and without contralateral noise. This block of stimuli thus yields a single measure of change analogous to the residual obtained for TEOAE measurement. Each of these results was subjected to the same noise rejection protocol described above. The stimulus blocks were repeated 32 times for a total of 512 pairs of probe presentations for the with- and without-contralateral noise conditions, yielding one subaverage. The measurement was repeated to obtain a second subaverage, doubling the total number of pairs of probe presentations (1024). Grand average “signal” and subtracted “noise” buffers were calculated as for the TEOAE measurements described above. Each measurement at a single contralateral noise level took  $\sim 3.5$  min.

Contralateral-noise-induced changes were detected above the measurement noise floor (typically  $\sim 20$ – $30$   $\mu\text{Pa}$  rms). Contralateral noise levels ranged from 30 to 100 dB SPL in increasing steps of 10 dB. The time averages were filtered using a FIR digital bandpass filter (software code from Agilent Technologies, Inc) and windowed by a recursive exponential window with 10 recursions (Shera and Zweig 1993). The spectra of

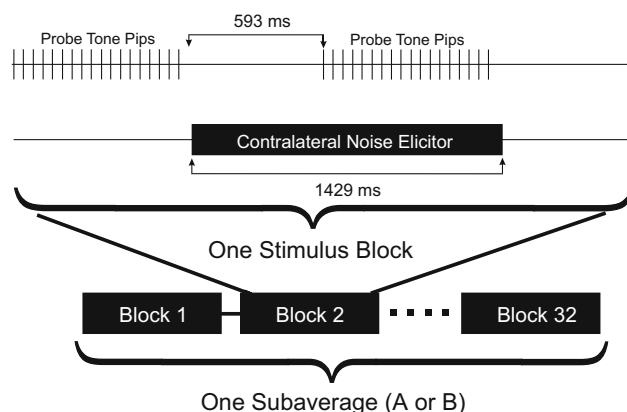


**FIG. 4.** Time record of stimulus probe tone pips and contralateral noise elicitor stimuli used to measure pressure changes related to MOCR and MEMR activation. As for TEOAE measurements, each stimulus block yielded one measure of the effect that was accepted only if it passed the noise rejection criteria. This sequence is repeated 32 times to calculate one of two subaverages.

<sup>2</sup> Subsequent to collecting data for this study, the averaging algorithm was modified to create the “signal” and “noise” buffers (A and B) using the results from individual stimulus blocks into alternating A and B “accumulator buffers” rather than separate sequential averages (for A and then B). This is likely to have further reduced the influence of slow drift.

the TEOAEs obtained using the scale-subtract method and the changes induced by contralateral noise were calculated using a 4096-point FFT performed on the time-domain responses.

Changes in the response to tone pip stimuli in the time interval of the stimulus pressure caused by contralateral noise are referred to as  $\Delta P_{\text{stim}}$ . Similarly, changes measured during the time delayed interval of the TEOAE are referred to as  $\Delta P_{\text{TEOAE}}$ . These changes, or residuals, were quantified in an appropriately chosen time window as the rms value of the signal and noise buffers for the TEOAE measurement and for each level of contralateral noise. Windows ranged from 1 to 6 ms (depending on stimulus frequency) centered on zero time for the stimulus interval and 6 to 12 ms centered on the delayed interval where the TEOAE was detected using the scale-subtract measurement. The sharply defined width of the recursive exponential windows, for which the time intervals outside the window have exactly zero amplitude (no side lobes in the time domain), made it easy to verify that the stimulus window contained only the stimulus pressure and the delayed window contained only the emission, including its components with the shortest measured delays. The time windows were fixed for all responses from the same subject for each probe frequency. Varying the width of the window can introduce artifacts in spectral analysis but has little effect on rms measurements of the time waveforms of  $\Delta P_{\text{stim}}$  and  $\Delta P_{\text{TEOAE}}$ .

Suppression presumed to result from either MEMR or MOCR activity was detected as a measurable change above the noise floor in either the stimulus and/or emission pressures. Changes in the stimulus interval ( $\Delta P_{\text{stim}}$ ) were readily detected as having time waveforms (observed visually online) and spectra (analyzed post hoc) similar to that of the stimuli and were taken as evidence that the middle ear reflex had been activated. Similarly, changes in the time interval of the emission ( $\Delta P_{\text{TEOAE}}$ ) resembled the emission, both in time waveform and spectrum. To be considered above threshold,  $\Delta P_{\text{stim}}$  or  $\Delta P_{\text{TEOAE}}$  was required to exceed the noise by at least 5 dB, corresponding to a reproducibility (correlation between the two time-domain subaverages expressed as a percentage (Kemp et al. 1986; Gorga et al. 1993)) of at least 50 %. We applied the same criteria to the total emission ( $P_{\text{TEOAE}}$ ). Attributing  $\Delta P_{\text{TEOAE}}$  in a given measurement exclusively to MOCR activation was only possible if there was no significant contamination by the MEMR as detected by a significant  $\Delta P_{\text{stim}}$  above the noise. In practice, displaying the signal and noise buffers online in the same plot greatly facilitates identifying a result very likely to be significant. If there was no effect of either efferent pathway, then the rms values of residuals in the signal buffer were

indistinguishable from that of the noise buffer, with random variations attributable to true system and subject noise. The approach of detecting  $\Delta P_{\text{stim}}$  and  $\Delta P_{\text{TEOAE}}$  is similar to that of Mertes and Goodman (2016) who used click stimuli instead of tone pips.

To provide a comparative conventional measure of the reflex threshold for the contralateral noise used in the TEOAE assessments, the tympanometer was set to acoustic reflex decay mode, so we could visually determine the threshold change in immittance while presenting the lab-generated contralateral noise instead of the on-board elicitor signal. The same attenuator was used to adjust the contralateral noise level as for the measurements of  $\Delta P_{\text{stim}}$  as described above.

## RESULTS

A complete set of data from one participant illustrates the results and the basis for interpretation (Fig. 5). Figure 5a shows time waveforms of the TEOAE in response to 3 kHz tone pips at 50 dB peSPL (70 dB peSPL reference) (black plot at the top of Fig. 5a) and changes induced by different levels of contralateral noise. Changes in  $\Delta P_{\text{TEOAE}}$  likely induced by the MOCR exceeded the threshold of 50 % reproducibility for contralateral noise levels of 50 dB and higher. Similarly,  $\Delta P_{\text{stim}}$  indicating activation of the MEMR exceeded 50 % reproducibility for contralateral noise levels of 90 and 100 dB SPL. In this example, the amplitude of  $\Delta P_{\text{TEOAE}}$  at the highest noise level that does not evoke the MEMR (80 dB SPL) is less than one fourth of the amplitude of the TEOAE (128.5 vs 573  $\mu\text{Pa}$  rms, respectively). Although  $\Delta P_{\text{TEOAE}}$  grows larger at higher noise levels, it is not possible to attribute this increase to greater activation of the MOCR because the MEMR is activated as well.

Spectral analysis of the time waveforms of Figure 5a also clearly reveals  $\Delta P_{\text{TEOAE}}$  for 50 dB SPL contralateral noise. The fine structure of the TEOAE amplitude and  $\Delta P_{\text{TEOAE}}$  are evident at this and higher levels of noise, demonstrating that the changes in this time interval induced by contralateral noise indeed represent changes in the amplitude of the TEOAE. The stimulus spectrum is also represented in this plot, allowing the relative levels of the stimulus, the emission, and  $\Delta P_{\text{TEOAE}}$  to be assessed. Spectral amplitudes are expressed in sound exposure level (SEL), which quantifies the sound level in one period of the repeated transient stimuli (Goodman et al. 2009). This measure thus depends on the presentation rate of the transients. (An alternate formulation that can be used to compare sound levels of transient stimuli of differing repetition period, including

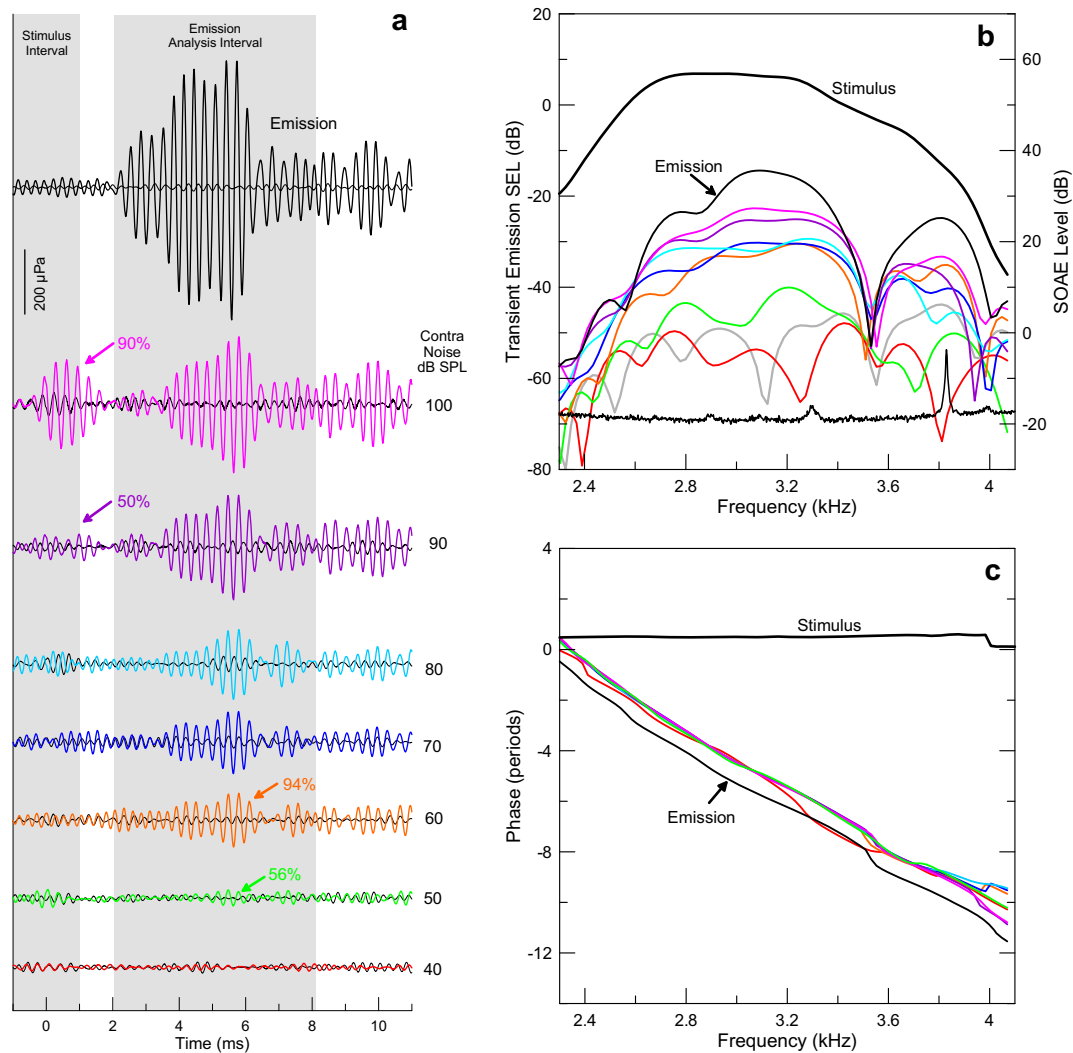


**FIG. 5.** Results from one participant (#28RF) illustrate the raw data. **a** Time waveforms of the TEOAE residual in response to 3 kHz tone pips at 50 dB peSPL (70 dB peSPL reference) (black plots at the top) and changes induced by different levels of contralateral noise are coded by color and the noise level is shown to the right of each plot. The 2-ms-wide shaded area centered on 0 ms represents the duration of the tone pip stimulus. The 6-ms-wide window centered on 5.1 ms represents the time window used to analyze the TEOAE and  $\Delta P_{\text{TEOAE}}$ . The thresholds for activating the MEMR and MOCR are 90 and 50 dB SPL contralateral noise as indicated by the purple and

green arrows, respectively. Reproducibility, indicated above the arrows, exceeded 50% at these and higher noise levels. **b** Spectral analysis of the time waveforms in panel a. The stimulus spectrum is also represented. The noise floor for the 40-dB SPL contralateral level is indicated as the gray curve. The spectral average at the bottom shows spontaneous emissions in this ear (level shown on the right y-axis). **c** The similarity in the slopes of the phase for the TEOAE and  $\Delta P_{\text{TEOAE}}$  reveals a similar group delay. The phase of the TEOAE has been shifted down by one period for comparison with phase of  $\Delta P_{\text{TEOAE}}$ .

chirps, normalizes the measure to a 1-s duration (Keefe et al. 2016). For our purpose, the duration does not matter because we wished to quantify the TEOAE relative to the transient stimulus that evoked it.) Spontaneous otoacoustic emissions (SOAEs) are present at 3.3 and 3.83 kHz in the 0.5-Hz resolution spectral average plotted at the bottom of Figure 5b. Peaks in the amplitude of the TEOAE and  $\Delta P_{\text{TEOAE}}$  near the frequencies of SOAEs are evident, even in a 6-ms analysis window near the end of the 46.44-ms buffer, confirming that the SOAEs were synchronized

by the tone pips. The stimulus interval that followed immediately was thus contaminated by the synchronized spontaneous otoacoustic emissions (SSOAEs). As others have reported, this contamination exists if an SSOAE does not desynchronize within one repetition period of the tone pips (46.44 ms). Minimizing the contamination of  $\Delta P_{\text{stim}}$  by SSOAEs requires either using a different probe frequency that does not synchronize the SOAEs or reducing its amplitude through filtering. Synchronous SOAEs are a problem to deal with online and this could be a limitation for

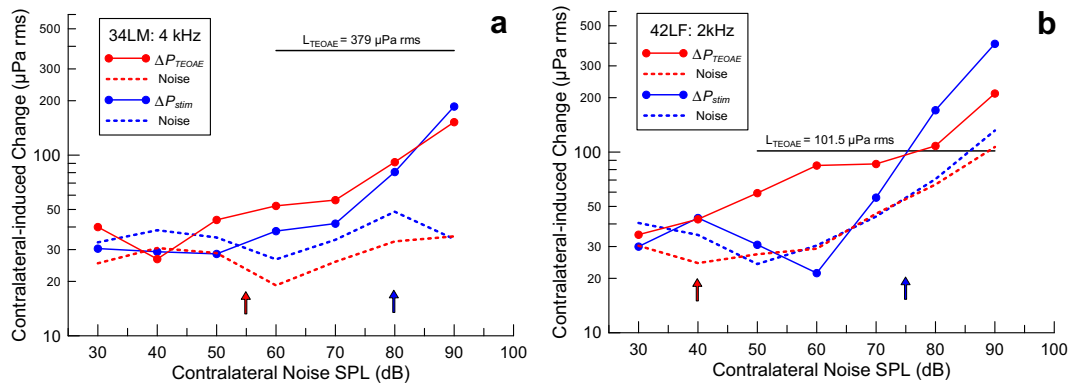


**FIG. 6.** Increasing contralateral noise levels reveals thresholds for  $\Delta P_{stim}$  (MEMR, blue) and  $\Delta P_{TEOAE}$  (MOCR, red). These examples show similar thresholds, but the degree of suppression of the TEOAE due to presumed MOCR activity is  $\sim 15\%$  for subject 34LM (a) and nearly complete ( $\sim 80\%$ ) for subject 42LF (b). The rms value of the TEOAE amplitude is indicated by the horizontal lines in each panel.

broadly adapting this measurement approach to characterize the thresholds of the two efferent pathways.

The similarity between the delay of the TEOAE and that of the changes induced by contralateral noise of 90 dBA or below (Fig. 5a) confirms that the primary effect of the noise is a selective effect on the TEOAE. This is demonstrated more clearly by the almost identical negative slope of the phase plots (group delay  $\sim 5.5$  ms) for both the TEOAE and changes in it induced by contralateral noise (Fig. 5c). The group delay of the contralateral-noise-induced change in the TEOAE does not change measurably even for the 100-dB SPL noise level where the MEMR is clearly active (Fig. 5a). Had we used an analysis window wide enough to include both the stimulus and emission time intervals, the phase would have shown irregularities due to mixing the short-latency  $\Delta P_{stim}$  with the longer-latency  $\Delta P_{TEOAE}$  similar to the phase irregularities reported by Guinan et al. (2003).

The two examples in Figure 6 show the dependence of  $\Delta P_{stim}$  and  $\Delta P_{TEOAE}$  on the level of contralateral noise for two subjects. The amplitude of the TEOAE, expressed in the same units as the change due to contralateral noise, is shown for reference. The two subjects show markedly different degrees of suppression of the TEOAE, presumably due to MOC activity: ( $\sim 15\%$ ) for subject 34LM (code indicates the Left ear of a Male) (Fig. 6a), and nearly complete ( $\sim 80\%$ ) suppression for subject 42LF (Fig. 6b). The measures of  $\Delta P_{stim}$  or  $\Delta P_{TEOAE}$  at several contralateral noise levels above threshold were used to establish the trend that allowed the contralateral noise threshold to be interpolated linearly to the nearest multiple of 5 dB. Note that  $\Delta P_{stim}$  in Figure 6b exceeds the amplitude of the TEOAE, as does  $\Delta P_{TEOAE}$  at the 90-dB noise level. This makes sense only as the result of activating the MEMR, since the probe stimulus pressure is on the order of 10 mPa rms, more than 80 times as large as the TEOAE it evokes.

Even a small change in eardrum impedance can account for such a large  $\Delta P_{stim}$ .

The results from all 10 subjects with complete sets of data are shown as signal-to-noise ratios vs contralateral noise level in Figure 7. All results from all 14 subjects are summarized individually in Table 1. The stimulus levels were well-controlled between subjects by our depth-compensated ear simulator calibration, so the large variability in  $\Delta P_{TEOAE}$  between subjects seen in Figure 7 is primarily due to a combination of variability in the emission levels and in the changes induced by contralateral noise. The noise floor for the lowest level of contralateral noise (30 dB SPL; below threshold for both  $\Delta P_{stim}$  and  $\Delta P_{TEOAE}$ ) was consistent between subjects, ranging between  $\sim 15$  and 30  $\mu\text{Pa}$  rms or about 6 dB. The largest value of  $\Delta P_{TEOAE}$  in the absence of an MEMR ( $\Delta P_{TEOAE\_max}$ ) ranged from 30.1 to 370  $\mu\text{Pa}$  ( $\sim 22$  dB) and  $P_{TEOAE}$  is about the same, ranging from 32 to 565.1  $\mu\text{Pa}$  ( $\sim 25$  dB). The greatest source of variability appears to be the emission generation process, not the noise floor including subject-generated noise. Even with this small sample size, it may be noteworthy that variability in  $\Delta P_{TEOAE\_max}$  was comparable to that of  $P_{TEOAE}$ , so the MOCR does not seem to contribute substantially to the variability in  $\Delta P_{TEOAE\_max}$  above that of the emission itself.

Consistent MEMR-mediated effects at contralateral noise levels above 70 dB SPL are readily apparent in the composite plot of Figure 7b, due to the relatively steep slope of the change in  $\Delta P_{stim}$  with increasing contralateral noise levels. This can be explained by the fact that the stimulus pressure is much larger than the emission pressure and even a small change in eardrum impedance can result in a large  $\Delta P_{stim}$ . The table shows that using  $\Delta P_{stim}$  to detect activation of the MEMR was more sensitive than the standard clinical test in all but one case. The conventional clinical MEMR threshold for contralateral noise averaged 92.1 dB SPL (SD 7.0 dB,  $N = 14$ ), compared



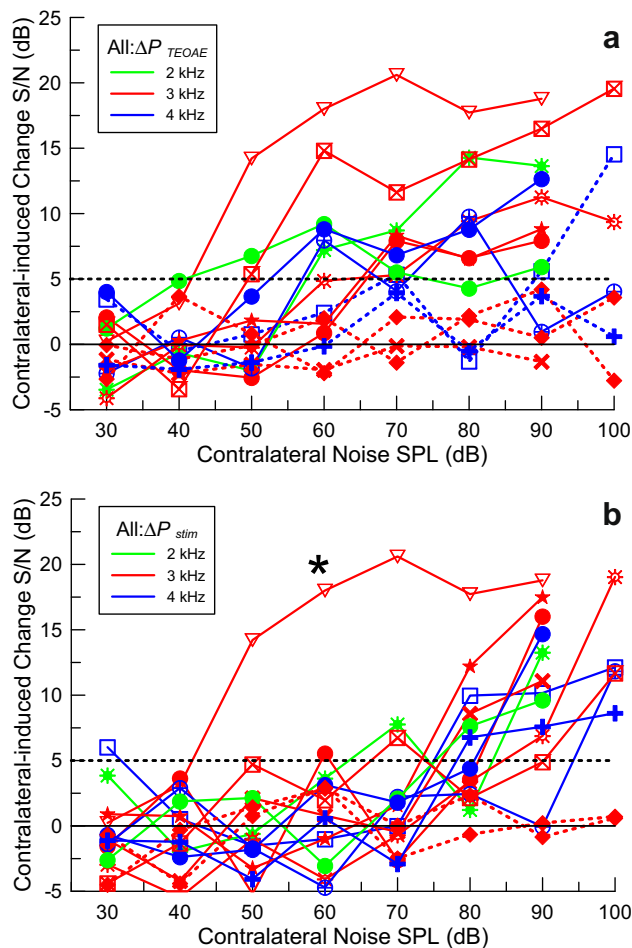


**FIG. 7.** Changes in S/N in all subjects for **a**  $\Delta P_{\text{TEOAE}}$  (MOCR) and **b**  $\Delta P_{\text{stim}}$  (MEMR) induced by contralateral noise coded by color for different probe frequencies with different symbols for each subject. The colored dashed curves show cases where the pressure change did not reach threshold (indicated with the black dashed horizontal line) for any level of contralateral noise. The plot marked with a star symbol in **b** is a case where synchronized spontaneous emissions contaminated the stimulus interval and it was not possible to measure the MEMR activation.

with a MEMR threshold measured using  $\Delta P_{\text{stim}}$  of 80.0 dB SPL (SD 8.4 dB,  $N = 11$ ). The threshold for  $\Delta P_{\text{stim}}$  averaged 11.0 dB (SD 5.7 dB) lower and this was highly significant (two-tailed  $t$  test;  $p = 0.0002$ ) for the 10 subjects with data for both measurements. The single curve marked with an asterisk is from a subject with strong SSOAEs that remained synchronized for the entire 46.44-ms repetition period of the probe stimuli and thus wrapped around into the next repetition. This obscured the stimulus interval and thus detecting the true  $\Delta P_{\text{stim}}$  was not possible. The reason that contralateral noise induced a change in the stimulus interval at low noise levels is because it suppressed the SSOAEs. In this example, it was not possible to remove the SSOAE artifact through filtering without also removing much of the TEOAE signal as well.

The level of contralateral noise to reach threshold for  $\Delta P_{\text{TEOAE}}$  was 56.7 dB (SD 8.3 dB,  $N = 10$ ). The difference in thresholds for  $\Delta P_{\text{stim}}$  and  $\Delta P_{\text{TEOAE}}$  was 23.9 dB (SD 12.4 dB,  $N = 9$ ) and highly significant (two-tailed  $t$  test;  $p = 0.0002$ ). No significant correlations were found between the amplitude of the TEOAE and the threshold for  $\Delta P_{\text{TEOAE}}$  or between the thresholds for  $\Delta P_{\text{stim}}$  and  $\Delta P_{\text{TEOAE}}$ . The behavioral threshold at the probe frequency ( $f_p$ ) negatively correlates with  $\log_{10}(P_{\text{TEOAE}})$  ( $R^2 = 0.33$ ,  $N = 14$ ,  $p = 0.016$ ) (Fig. 8a), where the TEOAE amplitude is denoted as  $P_{\text{TEOAE}}$ . This observation is consistent with the general finding that the levels of OAEs are larger in more sensitive ears. The suppression of the TEOAE by contralateral noise ( $(\Delta P_{\text{TEOAE}} - \Delta P_{\text{TEOAE}_{\text{max}}})/P_{\text{TEOAE}}$ ), expressed in decibels, was positively correlated with  $\log_{10}(P_{\text{TEOAE}})$  ( $R^2 = 0.56$ ,  $N = 10$ ,  $p = 0.012$ ) (Fig. 8b). This relation was also evaluated for  $\Delta P_{\text{TEOAE}}$  at a constant contralateral noise level of 70 dB ( $R^2 = 0.46$ ,  $N = 8$ ,  $p = 0.03$ ), but less so, possibly due to the loss of two subjects with thresholds for  $\Delta P_{\text{TEOAE}}$  that were either higher than 70 dB SPL (1 case) or where 70 dB SPL noise evoked the MEMR. Thus, the larger the amplitude of the emission, the less it was suppressed. A previous study found no correlation between the amplitudes of TEOAEs and the magnitude of suppression by contralateral sound (Hood et al. 1996). We have no explanation for this discrepancy.

## DISCUSSION

We have demonstrated that a simple measurement of time-domain averages of responses to tone pips using linear averaging can separately identify changes due to activation of the MEMR and MOC efferent pathways. With a suitable noise rejection algorithm, performed in real time, the method appears readily adaptable to laboratory research on humans and other species as well as to diagnostic tests in the hearing clinic. A recent report in mice using the same measurement system underscores the range of application of this approach (Xu et al. 2015, 2017). It is noteworthy that  $\Delta P_{\text{stim}}$  detects the effects of the MEMR at the frequency of probe tones in the range of 2–4 kHz (much higher in mice) and is not limited to the stiffness-dominated frequency range of middle ear transmission below 1 kHz (Keefe et al. 2010; Feeney et al. 2017). The presence of  $\Delta P_{\text{stim}}$  leaves little doubt that the interpretation of  $\Delta P_{\text{TEOAE}}$  is compromised by co-activation of the MEMR. It is thus not safe to assume that the effects of the MEMR are confined to low frequencies. In contrast, the absence of a measurable  $\Delta P_{\text{stim}}$  gives confidence that  $\Delta P_{\text{TEOAE}}$  has an inner ear origin, presumably due to MOCR activation. The relatively rapid interleaving with gated

TABLE 1

Compilation of results from all subjects with at least partial data sets. The subject code specifies a two-digit identification number, the ear (L/R) used for TEOAE measurements and sex (M/F). Data are missing when either the MEMR or MOCR threshold could not be measured

Subject code	Probe freq. (kHz)	Behavioral threshold SPL at $f_p$	Clinical MEMR Thr SPL	$\Delta P_{stim}^{MEMR}$ Thr SPL	$\Delta MEMR$ threshold (dB)	MOC threshold SPL	MEMR-MOC threshold (dB)	$P_{TEOAE}$ ( $\mu Pa$ rms)	$\Delta P_{TEOAE}^{re}$ $P_{TEOAE}$ (dB)	MOC suppression (dB)
42LF	2	10.2	90	75	15	40	35	122	-1.8	-14.4
87LF	2	15.0	80	85	-5	55	30	405	-15.6	-1.6
17LM	3	11.7	100	>100	-	-	-	155	-	-
28RF	3	13.2	100	85	15	50	35	566	-12.4	-2.4
36RM	3	11.2	100	-	-	-	-	65	-	-
59LF	3	17.5	90	70	20	-	-	33	-	-
62LF	3	17.9	90	75	15	60	15	76	-6.9	-5.2
73LF	3	15.8	90	80	10	60	20	43	-1.9	-14.0
77RM	3	12.1	100	85	15	60	25	142	-8.3	-4.2
82RM	3	4.8	90	-	-	45	-	579	-3.5	-9.5
13LF	4	12.8	90	75	15	-	-	85	-	-
34LM	4	4.9	80	80	0	55	30	393	-11.3	-2.75
65LF	4	17.3	100	85	15	55	30	88	-7.6	-4.7
72RM	4	9.8	90	75	15	70	5	615	-21.9	-0.7

contralateral noise is intended to optimize the detection of so-called fast efferent effects and is likely insensitive to slow efferent effects (Guinan et al. 2003). Averaging over the full time-course of the with- and without-contralateral noise intervals also likely minimizes contributions from intrinsic effects of prolonged presentation of the ipsilateral stimuli (Liberman et al. 1996). Consistent with this interpretation is the fact that the rms values of the signal and noise in  $\Delta P_{TEOAE}$  are indistinguishable at the lowest level of contralateral noise we used (30 dB SPL).

Linear averaging accurately measures the effect of contralateral noise on TEOAEs. Nonlinear TEOAE

extraction measurements may miss an important part of the phenomenon, although the degree of inaccuracy in estimating emission levels may not be large (Moleti et al. 2012). Components of SFOAE and TEOAE at a given frequency appear to originate basal to the resonant place on the basilar membrane, and exhibit more linear growth with stimulus level and shorter latency than components originating near the peak (Goodman et al. 2009; Moleti et al. 2014; Charaziak and Siegel 2015; Sisto et al. 2015). These short-latency components are removed by the nonlinear extraction, relative to later more compressive components. We are not able to address this issue directly in our data, as we used only linear averaging.

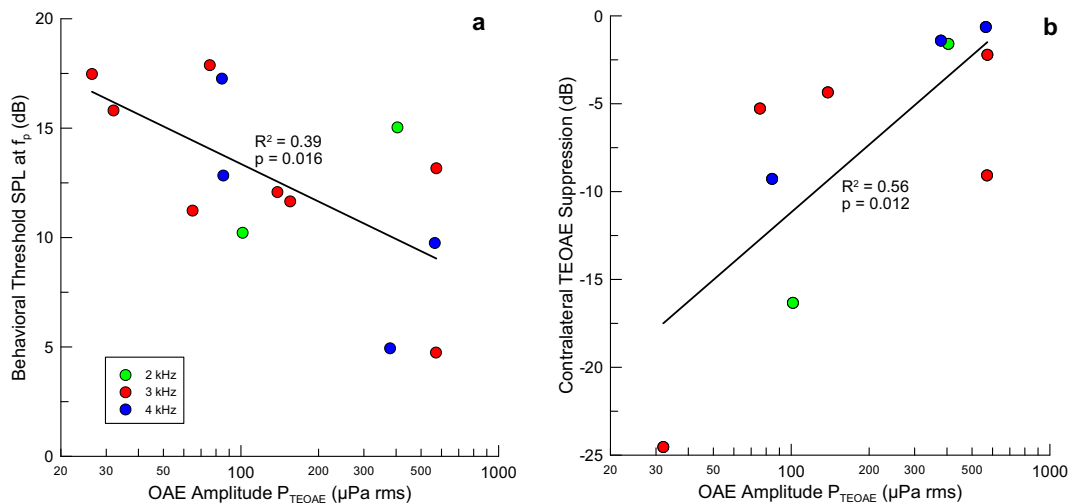


FIG. 8. The amplitude of TEOAEs correlated significantly with **a** behavioral thresholds at the probe frequency ( $N = 14$ ) and **b** the maximal change in emission amplitude induced by contralateral sound ( $\Delta P_{TEOAE\_max}$ ) relative to the amplitude of the emission ( $N = 10$ ).

### Conventional Clinical MEMR Tests Vs $\Delta P_{\text{stim}}$

In conventional clinical MEMR testing, a moderate-level, low-frequency probe tone (typically 226 Hz at 85 dB SPL or  $\sim 350$  mPa) and either an ipsilateral or contralateral tone or noise is used to elicit MEM contractions. During the test, the immittance at 226 Hz is displayed over time and the elicitor is presented at various levels until a change in immittance is detected as a deflection synchronized with the presentation of the elicitor. Assuming threshold would be assigned to a 10 % change in immittance, the corresponding pressure change would be approximately equivalent to a 65-dB tone or  $\sim 35$  mPa. Since the noise floor of measuring  $\Delta P_{\text{stim}}$  is about three orders of magnitude smaller, the onset of MEMR activity is considerably more sensitive than the clinical reflex test. The observation that the MEMR threshold in our participants determined clinically (using fairly coarse 10 dB resolution) averaged only 11.0 dB higher than our estimate using  $\Delta P_{\text{stim}}$  for the same contralateral noise is attributed to the steepness of the effect of MEMR activation with increasing noise level. We found no evidence for even a small degree of activation of the MEMR very much below the clinical threshold (at most 15 dB more sensitive in six cases). This statement should be cautioned by the small sample of clinically normal subjects in our study and previous reports of MEMR thresholds below 70 dB SPL, the lowest level at which the MEMR was detected in our sample. The 10–15-dB gain in sensitivity comes at the cost of the time required ( $\sim 3.5$  min of averaging for one contralateral noise level). Whether this increased sensitivity is justified over the much more rapid conventional MEMR testing seems questionable, unless there is a clear additional benefit. It might for example be useful for MEMR tests in individuals with unusually low loudness discomfort levels. Our test also shares the lack of a need to pressurize the ear canal with conventional MEMR testing and broadband reflectance measurement. Pressurization can be uncomfortable in some individuals and requires a tight seal that is difficult to achieve in some ears.

### Detecting when MOCR Measurements Are Contaminated by the MEMR

The approach described here compares favorably with other methods to detect activity of the two efferent pathways. A phase gradient method to detect contamination of discrete-tone-evoked SFOAEs relies on the presence of a component with very short delay, compared to the delay of the SFOAE itself (Guinan et al. 2003). Without decomposing the change in the SFOAE induced by the elicitor sound into components with short (MEMR) and long (MOCR) delay, a small contribution from the MEMR might be missed. When SFOAEs are evoked by discrete tones, this

method can be time-consuming, but SFOAEs measured using swept tones (Kalluri and Shera 2013) may require much less time to extract and better quantify the effects of MEMR and MOCR activity.

Other approaches rely on detecting the MEMR using a low-frequency stimulus, in the presence of OAEs evoked simultaneously at higher frequencies or SOAEs (i.e., Goodman and Keefe 2006; Deeter et al. 2009; Zhao and Dhar 2010, 2011). However, while changes in the response to the low-frequency stimulus induced by contralateral sound are very likely the result of the MEMR, it is not safe to assume that changes in the higher-frequency emissions are exclusively of MOCR origin. Our results demonstrate that the effects of the MEMR can extend above 1 kHz. In fact, the companion paper demonstrates MEMR effects above 20 kHz in mice (Xu et al. 2017), and separately reported in mice (for frequencies as high as 32 kHz) by Valero et al. (2016). Distortion product otoacoustic emissions (DPOAE) evoked by high-frequency stimuli in chinchillas were suppressed by low-frequency contralateral noise and suppression disappeared after sectioning the tendons of both middle ear muscles (Wolter et al. 2014). While this study did not measure changes in stimulus pressures caused by activating the MEMR, the only plausible explanation for this result is that the MEMR changed transmission through the middle ear of both the high-frequency stimuli and the DPOAE. Changes in primary levels in DPOAE measurements have been shown useful in detecting the MEMR (Henin et al. 2014). Large reductions in absorbance and absorbed power due to activating the MEMR with noise or tones were observed below 1 kHz in humans (Keefe et al. 2010; Feeney et al. 2017). These studies also measured small but consistent increases in absorbance and absorbed power between 1 and 4 kHz. In light of the larger changes at low frequencies, these changes at higher frequencies would be easy to overlook. But our study reveals that even these small changes due to activating the MEMR can produce changes in the amplitude of the stimulus pressure that are comparable to or larger than those caused by the MOCR.

Two studies that used acoustic clicks are more similar to the present report (Goodman et al. 2013; Boothalingam and Purcell 2015). Goodman et al. (2013) studied changes in TEOAEs induced by contralateral 30 or 60 dB SL white noise, presented for 30 s, interleaved by equal duration intervals without contralateral noise. The presence of both MOCR and MEMR were readily identified with great sensitivity using statistical resampling of the data obtained on individual trials to construct distributions of results with and without contralateral noise. The presence of any statistically significant change in the stimulus pressure was taken to mean that the MOC activity could not be interpreted cleanly. The long measurement intervals revealed slow drift in the levels

of individual time-windowed click stimuli that was addressed using detrending. Our results show that shortening the duration of the with- and without-contralateral noise intervals (1.43 s in our study) appears to substantially reduce the influence of drift reported by Goodman and colleagues, eliminating the need for post hoc detrending. We did not optimize this timing to minimize drift, so we do not claim that this is better than other durations. The changes in  $\Delta P_{\text{stim}}$  and  $\Delta P_{\text{TEOAE}}$  in the current study demonstrate directly how even near-threshold activation of the MEMR can produce a  $\Delta P_{\text{stim}}$  that grows rapidly and overwhelms the effect of the MOCR. While the study by Goodman and colleagues used the more time-consuming double-evoked OAE measurement method, Mertes and Goodman (2016) have evaluated the linear change induced by contralateral noise in the response to the lower-level clicks much as we have using tone pips. The measurements are both more time-efficient and also reveal changes in the whole emission, including components that may grow linearly with stimulus level (Backus and Guinan 2007; Mertes and Goodman 2016). Consistent with these studies, our data also reveal large differences in the size of the effects of the MOCR between individual subjects.

An approach similar to that of Goodman et al. (2013) also detected the MEMR using statistically significant changes in click level (Boothalingam and Purcell 2015). Although it is difficult to compare the methods used in these two studies with ours, the sensitivity to detect MEMR-induced changes appears comparable to ours. They both involved off-line data processing and artifact rejection, so it is hard to compare them directly. Our study directly revealed changes in the time intervals of the stimulus and emission while performing artifact rejection in real time. Only the quantification of rms signal and noise values in the two intervals was done off-line. Responses to individual transient stimuli were not retained in our study, so it is not possible to determine whether drift contributed to limiting the amplitude of the derived noise buffer. Still, despite being somewhat variable between participants, the noise measured in the ear was rarely much larger than the noise measured in a test cavity. This implies that drift was adequately rejected by the relatively short with- and without-noise intervals used to calculate  $\Delta P_{\text{stim}}$  and  $\Delta P_{\text{TEOAE}}$  for each stimulus block used to measure contralateral-noise-induced changes.

### Detecting when MEMR Measurements Are Contaminated by the MOCR

While our main concern was contamination of MOCR effects by the MEMR, it also appears that MEMR

measurements can be contaminated by MOCR-mediated changes to OAE sound pressure levels in the ear canal. Keefe et al. (2010, 2017) have questioned whether changes in ear canal pressure at low levels of a noise activator may be contaminated by the MOCR, leading to misinterpretation that the MEMR can have a threshold at 40 dB SPL or even lower. Consistent with this possibility, the spectrum of the change in canal pressure at low activator levels showed fine structure and marked changes in the spectrum that resemble that of TEOAEs and SFOAEs. This pattern was observed despite time windowing that restricted analysis to the first 2 ms after the click, excluding most of the TEOAEs that appear with a longer delay. We observed that long-lasting SSOAEs can wrap around into the next period of analysis from a preceding stimulus period (Fig. 7b). We demonstrated that SSOAEs can persist up to the end of the 46.44-ms buffer and had the same spectral content as the stimulus interval. It has been common practice to use even shorter interclick intervals to speed the TEOAE measurement and the effects of the MOCR, making it even more likely that SSOAEs could wrap into the next period. It would be interesting to examine whether ears with the lowest thresholds for MOCR activation also have long-lasting SSOAEs. SOAEs are more commonly seen between 1 and 2 kHz than for higher frequencies. Analyzing TEOAEs using windows centered on longer delays that are dominated by frequencies below 2 kHz may thus emphasize contributions of SSOAEs. Our experience is that this phenomenon may not compromise detecting MOCR effects, in agreement with previous reports (Marshall et al. 2014; Mertes and Goodman 2016). However, SSOAEs are quite variable between individual ears and this may have enhanced the between-subject variability of the measured effects of contralateral noise. This study shows that there is great variability even when SSOAEs are excluded, either by filtering or choosing a frequency for the probe tone pips that does not measurably synchronize SOAEs (Fig. 7). The upshot is that measurements of either MOCR or MEMR effects using ear canal pressure changes can be contaminated by the other efferent system. Methods like ours that can simultaneously identify activation of both pathways with equally high sensitivity can help minimize these problems.

### SUMMARY

We have demonstrated a simple method that measures changes in the ear canal pressure for transient stimuli induced by the MEMR and MOCR efferent pathways distinctly and directly. This method is



relatively immune to drift. Evoking the emissions using only the probe stimulus (i.e., without presenting interleaved reference pips) minimizes possible activation of the MOCR by the evoking stimuli. No assumptions are required as for separating the stimulus from the changes in the TEOAE induced by contralateral noise. However, the nonlinear compression method used to estimate the baseline TEOAE and the reference pips may have activated the ipsilateral MOCR to some unknown extent that will require further study. Both the ability to detect contaminating effects of the MEMR and the use of only low-level probe stimuli that do not activate the MEMR may improve the use of contralateral-noise-induced MOCR in diagnostic audiology. The method appears likely to be as reliable as other similar previously reported studies in humans. As the companion paper (Xu et al. 2017) demonstrates, it has also proven useful in measurements in awake mice.

## ACKNOWLEDGEMENTS

This study was funded by the Hugh Knowles Hearing Center and Northwestern University. We are very grateful for the thorough and helpful feedback from three anonymous reviewers.

## COMPLIANCE WITH ETHICAL STANDARDS

*Conflict of Interest* The authors declare that they have no conflict of interest.

## REFERENCES

- BACKUS BC (2007) Bias due to noise in otoacoustic emissions measurements. *J Acoust Soc Am* 121:1588–1603
- BACKUS BC, GUINAN JJ (2006) Time-course of the human medial olivocochlear reflex. *J Acoust Soc Am* 119:2889–2904
- BACKUS BC, GUINAN JJ (2007) Measurement of the distribution of medial olivocochlear acoustic reflex strengths across normal-hearing individuals via otoacoustic emissions. *J Assoc Res Otolaryngol* 8:484–496
- BOOTHALINGAM S, PURCELL DW (2015) Influence of the stimulus presentation rate on medial olivocochlear system assays. *J Acoust Soc Am* 137:724–732
- BORG E (1982) Time course of the human acoustic stapedius reflex: a comparison of eight different measures in normal-hearing subjects. *Scand Audiol* 11:237–242
- CHARAZIAK KK, SIEGEL JH (2015) Tuning of SFOAEs evoked by low-frequency tones is not compatible with localized emission generation. *J Assoc Res Otolaryngol* 16:317–329
- COLLET L, KEMP DT, VEUILLET E, DUCLAUX R, MOULIN A, MORGON A (1990) Effect of contralateral auditory stimuli on active cochlear micromechanical properties in human subjects. *Hear Res* 43:251–261
- COOPER NP, GUINAN JJ (2003) Separate mechanical processes underlie fast and slow effects of medial olivocochlear efferent activity. *J Physiol* 548:307–312
- DEETER R, ABEL R, CALANDRUCCIO L, DHAR S (2009) Contralateral acoustic stimulation alters the magnitude and phase of distortion product otoacoustic emissions. *J Acoust Soc Am* 126:2413–2424
- DELANO PH, ELGUEDA D, HAMAME CM, ROBLES L (2007) Selective attention to visual stimuli reduces cochlear sensitivity in chinchillas. *J Neurosci* 27:4146–4153
- DOLAN DF, GUO MH, NUTTALL AL (1997) Frequency-dependent enhancement of basilar membrane velocity during olivocochlear bundle stimulation. *J Acoust Soc Am* 102:3587–3596
- FEENEY MP, KEEFE DH, MARRYOTT LP (2003) Contralateral acoustic reflex thresholds for tonal activators using wideband energy reflectance and admittance. *J Speech Lang Hear Res* 46:128–136
- FEENEY MP, KEEFE DH, HUNTER, LL, FITZPATRICK DF, GARINIS AC, PUTTERMAN DB, McMILLAN GP (2017) Normative wideband reflectance, equivalent admittance at the tympanic membrane, and acoustic stapedius reflex threshold in adults. *Ear Hear* 38. doi:10.1097/AUD.0000000000000399
- GOODMAN SS, KEEFE DH (2006) Simultaneous measurement of noise-activated middle-ear muscle reflex and stimulus frequency otoacoustic emissions. *J Assoc Res Otolaryngol* 7:125–139
- GOODMAN SS, FITZPATRICK DF, ELLISON JC, JESTEADT W, KEEFE DH (2009) High-frequency click-evoked otoacoustic emissions and behavioral thresholds in humans. *J Acoust Soc Am* 125:1014–1032
- GOODMAN SS, MERTES IB, LEWIS JD, WEISSBECK DK (2013) Medial olivocochlear-induced transient-evoked otoacoustic emission amplitude shifts in individual subjects. *J Assoc Res Otolaryngol* 14:829–842
- GORGA MP, NEELY ST, BERGMAN BM, BEAUCHAINE KL, KAMINSKI JR, PETERS J, SCHULTE L, JESTEADT W (1993) A comparison of transient-evoked and distortion product otoacoustic emissions in normal-hearing and hearing-impaired subjects. *J Acoust Soc Am* 94:2639–2648
- GUINAN JJ (2006) Olivocochlear efferents: anatomy, physiology, function, and the measurement of efferent effects in humans. *Ear Hear* 27:589–607
- GUINAN JJ (2010) Cochlear efferent innervation and function. *Curr Opin Otolaryngol Head Neck Surg* 18:447–453
- GUINAN JJ JR, BACKUS BC, LILAONITKUL W, AHARONSON V (2003) Medial olivocochlear efferent reflex in humans: otoacoustic emission (OAE) measurement issues and the advantages of stimulus frequency OAEs. *J Assoc Res Otolaryngol* 4:521–540
- HENIN S, LONG GR, THOMPSON S (2014) Wideband detection of middle ear muscle activation using swept-tone distortion product otoacoustic emissions. *J Acoust Soc Am* 136:272–283
- HOOD LJ, BERLIN CI, BORDELON J, ROSE K (2003) Patients with auditory neuropathy/dys-synchrony lack efferent suppression of transient evoked otoacoustic emissions. *J Am Acad Audiol* 14:302–313
- HOOD LJ, BERLIN CI, HURLEY A, CECOLA RP, BELL B (1996) Contralateral suppression of transient-evoked otoacoustic emissions in humans: intensity effects. *Hear Res* 101:113–118
- KALLURI R, SHERA CA (2007) Comparing stimulus-frequency otoacoustic emissions measured by compression, suppression, and spectral smoothing. *J Acoust Soc Am* 122:3562–3575
- KALLURI R, SHERA CA (2013) Measuring stimulus-frequency otoacoustic emissions using swept tones. *J Acoust Soc Am* 134:356–368
- KEEFE DH, FITZPATRICK D, LIU Y-W, SANFORD CA, GORGA MP (2010) Wideband acoustic-reflex test in a test battery to predict middle ear dysfunction. *Hear Res* 263:52–65
- KEEFE DH, FEENEY MP, HUNTER LL, FITZPATRICK DF (2016) Comparisons of transient evoked otoacoustic emissions using chirp and click stimuli. *J Acoust Soc Am* 140:1949–1973

- KEEFE DH, FEENEY MP, HUNTER LL, FITZPATRICK DF (2017) Aural acoustic stapedius-muscle reflex threshold procedures to test human infants and adults. *J Assoc Res Otolaryngol* 18:65–88
- KEMP DT, CHUM R (1980) Properties of the generator of stimulated acoustic emissions. *Hear Res* 2:213–232
- KEMP DT, BRAY P, ALEXANDER L, BROWN AM (1986) Acoustic emission cochleography—practical aspects. *Scand Audiol Suppl* 25:71–95
- KEMP DT, RYAN S, BRAY P (1990) A guide to the effective use of otoacoustic emissions. *Ear Hear* 11:93–105
- LEE J, DHAR S, ABEL R, BANAKIS R, GROLLEY E, LEE J, ZECKER S, SIEGEL JH (2012) Behavioral hearing thresholds between 0.125 and 20 kHz using depth-compensated ear simulator calibration. *Ear Hear* 33:315–329
- LIBERMAN MC, PURIA S, GUINAN JJ JR (1996) The ipsilaterally evoked olivocochlear reflex causes rapid adaptation of the  $2 f_1-f_2$  distortion product otoacoustic emission. *J Acoust Soc Am* 99:3572–3583
- LIBERMAN MC, LIBERMAN LD, MAISON SF (2014) Efferent feedback slows cochlear aging. *J Neurosci* 34:4599–4607
- MAISON SF, LIBERMAN MC (2000) Predicting vulnerability to acoustic injury with a noninvasive assay of olivocochlear reflex strength. *J Neurosci* 20:4701–4707
- MAISON SF, USUBUCHI H, LIBERMAN MC (2013) Efferent feedback minimizes cochlear neuropathy from moderate noise exposure. *J Neurosci* 33:5542–5552
- MARKS K, SIEGEL JH (2011) Separating olivocochlear and acoustic reflex actions on otoacoustic emissions in the time domain. *Assoc Res Otolaryngol Abst* 34:125
- MARSHALL L, LAPSLEY MILLER JA, GUINAN JJ, SHERA CA, REED CM, PEREZ ZD, DELHORNE LA, BOEGE P (2014) Otoacoustic-emission-based medial-olivocochlear reflex assays for humans. *J Acoust Soc Am* 136:2697–2713
- MERTES IB, GOODMAN SS (2016) Within- and across-subject variability of repeated measurements of medial olivocochlear-induced changes in transient-evoked otoacoustic emissions. *Ear Hear* 37:e72–e84
- MOLETTI A, BOTTI T, SISTO R (2012) Transient-evoked otoacoustic emission generators in a nonlinear cochlea. *J Acoust Soc Am* 131:2891–2903
- MOLETTI A, SISTO R, LUCERTINI M (2014) Experimental evidence for the basal generation place of the short-latency transient-evoked otoacoustic emissions. *J Acoust Soc Am* 135:2862–2872
- MØLLER AR (2012) Acoustic middle ear reflex. In: *Hearing anatomy, physiology, and disorders of the auditory system*. Plural Publ, San Diego, pp 241–256
- MOUNTAIN DC (1980) Changes in endolymphatic potential and crossed olivocochlear bundle stimulation alter cochlear mechanics. *Science* 210:71–72
- MURUGASU E, RUSSELL IJ (1996) The effect of efferent stimulation on basilar membrane displacement in the basal turn of the guinea pig cochlea. *J Neurosci* 16:325–332
- NEELY ST, LIU Z (1994) EMAY: otoacoustic emission averager. Technical Memo No. 17. Boys Town National Research Hospital, Omaha
- NEELY ST, STEVENSON R (2002) SysRes. Technical Memo No. 19. Boys Town National Research Hospital, Omaha
- RASETSHWANE DM, NEELY ST (2011) Calibration of otoacoustic emission probe microphones. *J Acoust Soc Am* 130:EL238
- RELKIN EM, STERNS A, AZEREDO W, PRIEVE BA, WOODS CI (2005) Physiological mechanisms of onset adaptation and contralateral suppression of DPOAEs in the rat. *J Assoc Res Otolaryngol* 6:119–135
- ROBLES L, DELANO PH (2008) Efferent system. In: Dallos P, Oertel D (eds) *The senses: a comprehensive reference*. Academic, London, pp 413–445
- SHERA CA, ZWEIG G (1993) Noninvasive measurement of the cochlear traveling-wave ratio. *J Acoust Soc Am* 93:3333–3352
- SIEGEL JH (2002) Calibrating otoacoustic emission probes. In: Robinette MS, Glatke TJ (eds) *Otoacoustic emissions: clinical applications*, 3rd edn. Thieme Medical, New York, pp 416–441
- SIEGEL JH, KIM DO (1982) Efferent neural control of cochlear mechanics? Olivocochlear bundle stimulation affects cochlear biomechanical nonlinearity. *Hear Res* 6:171–182
- SIEGEL JH, CHARAZIAK K, CHEATHAM MA (2011) Transient- and tone-evoked otoacoustic emissions in three species. *AIP Conf Proc* 1403:307–314
- SISTO R, MOLETTI A, SHERA CA (2015) On the spatial distribution of the reflection sources of different latency components of otoacoustic emissions. *J Acoust Soc Am* 137:768–776
- SONGER JE, ROSOWSKI JJ (2005) The effect of superior canal dehiscence on cochlear potential in response to air-conducted stimuli in chinchilla. *Hear Res* 210:53–62
- SOUZA N, DHAR S, NEELY ST, SIEGEL JH (2014) Comparison of nine methods to estimate ear-canal stimulus levels. *J Acoust Soc Am* 136:1768–1787
- VALERO MD, HANCOCK KE, LIBERMAN MC (2016) The middle ear muscle reflex in the diagnosis of cochlear neuropathy. *Hear Res* 332:29–38
- WHITEHEAD ML, MARTIN GK, LONSBURY-MARTIN BL (1991) Effects of the crossed acoustic reflex on distortion-product otoacoustic emissions in awake rabbits. *Hear Res* 51:55–72
- WINSLOW RL, SACHS MB (1987) Effect of electrical stimulation of the crossed olivocochlear bundle on auditory nerve response to tones in noise. *J Neurophysiol* 57:1002–1021
- WOLTER NE, HARRISON RV, JAMES JL (2014) Separating the contributions of olivocochlear and middle ear muscle reflexes in modulation of distortion product otoacoustic emission levels. *Audiol Neurotol* 19:41–48
- XU Y, CHEATHAM MA, SIEGEL JH (2015) Separating medial olivocochlear from acoustic reflex effects on transient evoked otoacoustic emissions in unanesthetized mice. In: *Proceedings of the 12th international mechanics of hearing workshop*. Date: 23–29 June 2014 Location: Cape Sounio, Greece. Edited by DP Corey and KD Karavtiki. AIP conf. proc. 1703:090026
- XU Y, CHEATHAM MA, SIEGEL JH (2017) Identifying the origin of effects of contralateral noise on transient evoked otoacoustic emissions in unanesthetized mice. *J Assoc Res Otolaryngol*. doi:10.1007/s10162-017-0616-x
- ZHAO W, DHAR S (2010) The effect of contralateral acoustic stimulation on spontaneous otoacoustic emissions. *J Assoc Res Otolaryngol* 11:53–67
- ZHAO W, DHAR S (2011) Fast and slow effects of medial olivocochlear efferent activity in humans. *PLoS One* 6:e18725